

# Multi-area Economic Dispatch with GUPFC using Improved Bat Algorithm

S.Vijayaraj\* and R. K. Santhi

Research Scholar,  
Department of Electrical and Electronics Engineering,  
Annamalai University,  
Chidambaram.

Professor,  
Department of Electrical and Electronics Engineering,  
Annamalai University,  
Chidambaram.

\*Corresponding author's email: veejay\_raj [AT] yahoo.co.in

---

**ABSTRACT**— *This paper presents an Improved bat algorithm for the multi area multi-fuel economic–emission dispatch problem. it implements many objectives to be better concealed by in operation constraints and device limits. The formulation of practical generation cost consists cost of reactive power generation, shunt power injections, and total power losses, along with the conventional active power generation cost. An objective based on the concept of multi-fuel emissions makes the problem more practical, and a generalized unified power flow controller (GUPFC) is considered. An improved bat algorithm is used to solve the multi-objective problem on the standard IEEE-30 bus.*

**Keywords**— GUPFC, Multi-fuel active power cost, Multi-fuel reactive power cost Multi-fuel emissions, GUPFC installation cost, Transmission loss, Improved bat algorithm.

---

## 1. INTRODUCTION

In today's situation electric power system and their operation are among the most complex issues due to profoundly non-direct and computationally troublesome situations. The essential target in the arranging furthermore, operation of power systems is to give quality power supply to consumers at an efficient expense. The expanding energy demand and the diminishing energy resources have made an incredible need in power system operation and arranging. Economic Dispatch (ED) is the improvement plan of an generation system to compute the best generation schedule to supply a predetermined given load at a minimum cost while satisfying the essential constraints like power balance, generation limits constraint and tie-line constraint.

The calculation of optimum generation schedules for predicted loads over a period of time with due considerations of generator ramping rate limits, non-smooth fuel cost function due to the valve-point effect, multi fuel options and prohibitive operating zones leads to an advanced economic dispatch with multiple objectives and several constraints, effectively termed as multi-constrained dynamic economic dispatch.

Right now, with expanding attention to ecological contamination brought on by the blazing of fossil powers, the emanation of toxins is likewise a measure for the economic dispatch of the power plants. The environmental objective of the generation dispatch is to minimize the aggregate ecological expense or the aggregate contamination outflow. As of late, the issue which has pulled in much consideration, is contamination minimization because of the squeezing open interest for clean air. Thermal power stations are real reasons for environmental contamination, because of the high centralization of toxins transmitted. The reason for Emission Constrained Economic Dispatch (ECED) is to get the ideal generation plan by minimizing the fuel expense and emission level all the while fulfilling the load demand and operational limitations.

Electric power systems are interconnected because of the way that it is better to work them with more unwavering quality, enhanced security and less generation cost than the isolated systems. Multi-Area Economic Dispatch (MAED) is an advancement plan to decide the generation schedule plan for a given burden at the very least cost, while fulfilling power equalization, generator utmost and tie-line security limitations.

The objective of the Optimal Power Flow program is to furnish the electric utility with set focuses to enhance the present power system state regarding different targets, for example, minimization of the total generation cost, minimization of the total active power network misfortunes and amplification of the level of security. The Multi-area Optimal Power Flow (MOPF) issue is an extensive scale non-direct improvement issue with both linear and nonlinear

requirements. multi-area OPF estimations decide the ideal generation plan, ideal control variables and system quantities of each area of every area with due thought of generation and transmission framework confinements.

Song et al [1] proposed a direct programming based methodology applied to dynamic load dispatch of electric power systems considering security and environment requirements. Notwithstanding the fundamental limitations, such as generator real power limits and real power demand, a thorough arrangement of limitations are considered including transmission line limits, generators dynamic ramp rate, voltage security edge and/or natural issues. Voltage security edge is considered heuristically through the control of transmission line limits amid the arrangement procedure.

Shoultz et al[2] presented a strategy for unit commitment and multi-area economic dispatch with import/trade requirements. The authors proposed the traditional economic dispatch technique for tackling the multi- area economic dispatch issue. For the multi-area economic dispatch, the region incremental fuel expense was initially decided and after that the generator yields of units in every area were resolved.

Wang and Shahidehpour [3] proposed a deterioration approach for settling multi- area generation scheduling with tie-line imperatives utilizing expert systems. The authors demonstrated the efficiency of their methodology by testing it on a four area system with every area comprising of 26 units. Wang and Shahidehpour [4] likewise reported a large scale system decay and co-ordination strategy for the multi- area generation scheduling of hydrothermal systems with tie-line requirements.

Streiffert et al [5] detailed a multi-range ED issue as a limit non-linear network flow issue. The author exhibited another method utilizing an incremental network flow programming calculation. The method was quick, powerful and extensible to vast scale multi-area ED issues.

There has been a lot of examination on the assurance of optimal power flow (OPF) for different power system objectives, for example, the era cost, emanations, and transmission misfortunes (see, for instance, [6–14] for individual goals, and [15–20] for single-zone area multi-objective systems). A number of ways to deal with the multi-area economic dispatch issue under different power system working limitations are talked about in [21–25].

Lai et al [26] proposed the utilization of evolutionary programming to tackle the ideal power flow problem with Flexible AC Transmission Frameworks (FACTS). The Unified Power Flow Controller (UPFC) is utilized as a phase shifter and/or series compensator to manage both the angles and the magnitude of branch voltages. The calculation figures the ideal arrangement of base case and contingency case of the IEEE 30-bus system.

Prassana et al [27] connected two new computationally efficient enhanced stochastic calculations for tackling OPF of interconnected power systems with FACTS devices. These proposed calculations (FMPEP and FGTS) depend on the use of fuzzy logic technique fused in both EP and TS calculations. Different FACTS devices were incorporated into OPF in particular Static Var Compensator (SVC), Static Synchronous Compensator (STATCOM), Thyristor Controlled Series Capacitor (TCSC), and Unified Power Flow Controller (UPFC). The ideal solutions acquired utilizing EP, TS, FMPEP and FGTS are compared and analysed. The analysis reveals that the proposed calculations are generally straightforward, efficient and dependable.

Innovative improvements in the power semiconductor industry, and applications in AC transmission frameworks, have offered ascend to the requirement for another era of adaptable flexible AC transmission system (FACTS) devices. Most thinks about focus on unified power flow controller (UPFC) modeling procedures [28–30], ideal location approaches [31–33], and different control techniques to work UPFC [34]. Notwithstanding, the nature of its development implies that UPFC can't control various lines.

By and by, controlling different transmission lines is desirable over controlling only one transmission line. To perform multi- line control operations, we consider one of the new generations of convertible static compensators. This controller, which comprises of two or more arrangement converters composed with one shunt converter, is known as a generalized unified power flow controller (GUPFC).

Lubis, R.S et al [35] proposed a straight forward GUPFC model, which considered a nonlinear predictor–corrector primal-double inside point OPF without converter switching losses. A straightforward quadratic cost function was upgraded to fulfill equality and inequality constraints. The literature concerning the OPF problem in the presence of FACTS controllers is presented in [36-44].

Dandachi, N.H et al [45] estimated the reactive power production cost by considering reactive power cost curves. Wills, L et al [46] gives decomposition of the real and reactive power prices are into the generation cost and the transmission losses. Lamont, J.W et al [47] solved The optimal reactive power dispatch, in terms of optimal allocation and generation of reactive power required by the load centers is based on the real-time operating conditions. A careful survey of the writing uncovers that the expense of reactive power, losses, and the reactive power of shunt compensators ought to be considered to build the viability and reality of the OPF issue.

In this paper, our objective is to minimize the generation cost, emission level and total transmission power loss. An Improved bat algorithm is proposed to enhance the optimization. multi-fuel active and reactive power costs are formulated, along with the costs of reactive power generated by the shunt capacitors and total power losses to make realistic. To optimize the stated objectives, a complete power injection model of the GUPFC is taken from [48]. The effectiveness of the proposed method is tested on IEEE-30 bus test systems.

## 2. GUPFC POWER INJECTION MODELLING

Normally, a GUPFC consists of two or more series converters and one shunt converter. To illustrate the control operation of GUPFC, Fig. 1 shows two series converters coordinated with one shunt converter. To install a GUPFC, we require two lines with a common bus. For a given system, installing the device in lines connected to PV buses is far less effective than using lines connected to PQ buses. Hence, to reduce the number of possible locations and execution time, we consider the following rules. The GUPFC should be located between two PQ buses, and there should not be any shunt capacitors. The GUPFC should not be placed in the same line as a tap-changing transformer [52].

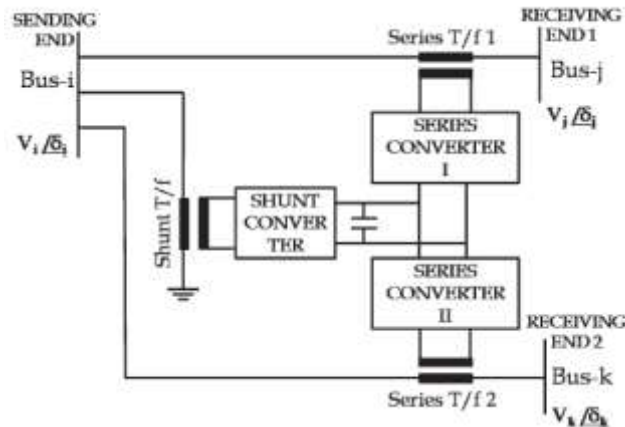


Fig. 1 GUPFC with two series converters

The complete power injection model with power mismatch and Jacobian elements is given in “Appendix”. The final steady-state power injection model of a GUPFC is shown in Fig. 2.

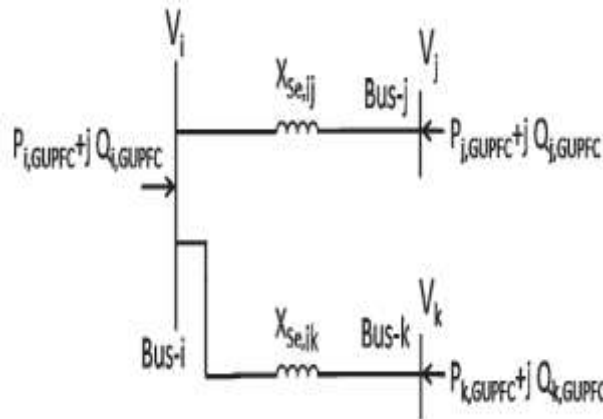


Fig. 2. steady-state power injection model of a GUPFC

The injected active and reactive powers can be expressed as

$$P_{i,GUPFC} = -V_i^2 \left[ \sum_{q=j,k} r_{iq} B_{se,iq} \sin \gamma_{iq} \right] - 1.0 \left( \sum_{q=j,k} r_{iq} V_i V_q B_{se,iq} \sin(\delta_{iq} + \gamma_{iq}) - r_{iq} V_i^2 B_{se,iq} \sin \gamma \right) \quad (1)$$

$$Q_{i,GUPFC} = -V_i^2 \left[ \sum_{q=j,k} r_{iq} B_{se,iq} \cos \gamma_{iq} \right] + Q_{sh} \quad (2)$$

$$P_{p,GUPFC} = r_{ip} V_i V_p B_{se,ip} \sin \sin(\delta_{iq} + \gamma_{iq}) \quad \forall p = j, k \quad (3)$$

$$Q_{p,GUPFC} = r_{ip} V_i V_p B_{se,ip} \cos \cos(\delta_{iq} + \gamma_{iq}) \quad \forall p = j, k \quad (4)$$

where  $r$  and  $\gamma$  are the per unit magnitude and phase angles, respectively, of the series voltage sources operating within the limits  $0 \leq r \leq r_{max}$  and  $0 \leq \gamma \leq \gamma_{max}$ .  $B_{se}$  is the susceptance of the series-connected converter transformer. The procedure to incorporate the GUPFC in the Newton– Raphson method follows that described in [30,31].

### 2.1. Investment cost

Generally, a UPFC can be considered as a combination of a static compensator (STATCOM) and static synchronous series compensator (SSSC). Similarly, a GUPFC combines a UPFC and SSSC. Hence, the investment cost (IC) of GUPFC can be considered as the sum of the investment costs of UPFC and SSSC and the operating range of UPFC in

MVar is  $S_{UPFC} = |Q2| - |Q1|$ , where  $Q1$ ,  $Q2$  are the reactive power flows in the line before and after placing the UPFC. Similarly, the IC of SSSC is

$$IC_{GUPFC} = IC_{UPFC} + IC_{SSSC} \quad (5)$$

The IC of UPFC [52] over a period of 15 years can be given as

$$IC_{UPFC} = \frac{C_{UPFC} \times S_{UPFC} \times 1000}{15 \times 8760} \$/h \quad (6)$$

Here, the installation cost of UPFC is

$$C_{UPFC} = 0.0003S_{UPFC}^2 - 0.2691S_{UPFC} + 188.22 \$/kVar$$

Similarly, the IC of SSSC [53] is

$$IC_{SSSC} = \frac{S_{SSSC} \times \eta \times CRF}{15 \times 8760} \$/h \quad (7)$$

where the capital recovery factor (CRF) =  $\frac{1(1+i)^n}{1(1+i)^n - 1}$  for discount rate 'i' (6%) and investment cost coefficient  $\eta$  (50,000 \$/MVA).

## 2.2. Optimal location

The spot at which the device is introduced will improve the framework security by minimizing either the line stacking or the bus voltage limit burdening under possibility operations. The system severity function (FSeverity) can be defined as [33]

$$F_{Severity} = \sum_{i=1}^{N_{line}} \left( \frac{S_i}{S_i^{max}} \right)^{2q} + \sum_{j=1}^{N_{bus}} \left( \frac{V_{j,ref} - V_j}{V_{j,ref}} \right)^{2r} \quad (8)$$

where  $N_{line}$ ,  $N_{bus}$  are the total number of lines and buses in a given system,  $S_i$ ,  $S_i^{max}$  are the present and maximum apparent powers of the  $i_{th}$  line,  $V_{j,ref}$ ,  $V_j$  are the nominal and present voltage values at the  $j_{th}$  bus, and  $q$ ,  $r$  are coefficients used to penalize overloads and voltage violations. These parameters are assigned a value of 2.

To upgrade system security under contingencies, the GUPFC apparatus ought to be set in a suitable location. At first, contingency analysis is performed by expelling a single transmission line at once and recognizing the quantity of voltage violation buses (NVVB) and number of overloaded lines (NOLL). The performance index is ascertained by summing NVVB and NOLL. At long last, the contingency with the most highest performance index value is recognized as the most basic.

This basic line is then expelled from the framework, and the GUPFC is put in one of the conceivable establishment locations examined in Sect. 2. At every conceivable area, the severity function  $F_{Severity}$  is minimized subject to certain viable requirements and device control settings. At last, the area with the least severity rate is recognized, and the GUPFC is introduced at this point.

## 3. PROBLEM FORMULATION

Normally, the objective of the OPF issue is to recognize an arrangement of control variables that improve certain power system targets while fulfilling practical constraints and FACTS device limits.

The OPF problem can be mathematically formulated as:

$$\text{Min } J(x,u) \text{ s.t. } g(x,u) = 0 \text{ and } h(x,u) \leq 0 \quad (9)$$

where  $g$  and  $h$  are equality and inequality constraints,

respectively.  $x$  is the state vector of dependent variables, such as slack bus active power generation ( $P_{g1}$ ), load bus voltage magnitudes ( $V_l$ ), generator reactive power output ( $Q_g$ ), and apparent power flow ( $S_{line}$ ).  $u$  is the control vector of independent variables (control variables), such as the generator active power output ( $P_g$ ), generator voltage ( $V_g$ ), transformer tap ratios ( $T$ ), and the reactive power output of VAr sources ( $Q_{sh}$ ).

The state and control vectors can be mathematically expressed as

$$x^T = [P_{g1}, V_{l1}, \dots, V_{lnl}, Q_{g1}, \dots, Q_{gNG}, S_{l1}, \dots, S_{lnl}] \quad (10)$$

$$u^T = [P_{g2}, \dots, P_{gNG}, V_{g1}, \dots, V_{gNG}, Q_{sh1}, \dots, Q_{shnc}, T_1, \dots, T_{nt}] \quad (11)$$

where  $NL$ ,  $NG$ ,  $nl$ ,  $nc$ , and  $nt$  are the total number of load buses, generator buses, transmission lines, VAr sources, and regulating transformers, respectively. The above problem is optimized by satisfying the following constraints.

### 3.1. Equality constraints

These constraints are typically load flow equations for multiple areas:

$$P_{g,k} - P_{d,k} - \sum_{m=1}^{m=N_{bus}} |V_k| |V_m| |Y_{km}| \cos(\theta_{km} - \delta_k + \delta_m) = 0 \quad (12)$$

$$Q_{g,k} - Q_{d,k} - \sum_{m=1}^{m=N_{bus}} |V_k| |V_m| |Y_{km}| \sin(\theta_{km} - \delta_k + \delta_m) = 0 \quad (13)$$

where  $P_{gk}$ ,  $Q_{gk}$  are the active and reactive power generation at the  $k_{th}$  bus,  $P_{dk}$ ,  $Q_{dk}$  are the active and reactive power demands at the  $k_{th}$  bus,  $|V_k|$ ,  $|V_m|$  are the voltage magnitudes at the  $k_{th}$  and  $m_{th}$  buses,  $\delta_k$ ,  $\delta_m$  are the phase angles of the voltage at the  $k_{th}$  and  $m_{th}$  buses, and  $|Y_{km}|$ ,  $\theta_{km}$  are the bus admittance magnitude and its angle between the  $k_{th}$  and  $m_{th}$  buses.

### 3.2. Inequality constraints

Generator bus voltage limits:

$$V_{G_i}^{min} \leq V_{G_i} \leq V_{G_i}^{max} \quad \forall i \in NG \quad (14)$$

Active power generation limits:

$$P_{G_i}^{min} \leq P_{G_i} \leq P_{G_i}^{max} \quad \forall i \in NG \quad (15)$$

Transformer tap setting limits

$$T_i^{min} \leq T_i \leq T_i^{max} \quad \forall i \in NT \quad (16)$$

Capacitor reactive power generation limits:

$$Q_{sh_i}^{min} \leq Q_{sh_i} \leq Q_{sh_i}^{max} \quad \forall i \in NC \quad (17)$$

Transmission line flow limit:

$$S_i \leq S_i^{max} \quad \forall i \in NG \quad (18)$$

Reactive power generation limits:

$$Q_{G_i}^{min} \leq Q_{G_i} \leq Q_{G_i}^{max} \quad \forall i \in NG \quad (19)$$

Load bus voltage magnitude limits:

$$V_i^{min} \leq V_i \leq V_i^{max} \quad \forall i \in NL \quad (20)$$

The control variables in this problem are self-constrained, whereas the inequality constraints such as  $P_{g1}$ ,  $V_i$ ,  $Q_{gi}$ , and  $S_{li}$  are non-self-constrained by nature. Hence, these inequalities are incorporated into the objective function using a penalty approach [57]. The augmented function can be formulated as:

$$J_{aug}(x, u) = J(x, u) + R_1 (P_{g1} - P_{g1}^{lim})^2 + R_2 \sum_{i=1}^{i=NL} (V_i - V_i^{lim})^2 + R_3 \sum_{i=1}^{i=NG} (Q_{gi} - Q_{gi}^{lim})^2 + R_4 \sum_{i=1}^{i=nl} (S_{li} - S_{li}^{max})^2 \quad (21)$$

where  $R_1$ ,  $R_2$ ,  $R_3$ , and  $R_4$  are the penalty quotients, which take large positive values. The limit values of the dependent variable  $x^{lim}$  can be given as:

$$x^{lim} = \begin{cases} x, x^{min} \leq x \leq x^{max} \\ x^{max}, x \geq x^{max} \\ x^{min}, x \leq x^{min} \end{cases} \quad (22)$$

### 3.3. Prohibited operating zones (poz):

In practice, when adjusting the output of a generator unit, it is important to avoid operating in prohibited zones so that the thermal unit efficiency can be maintained during vibrations in the shaft or other machine faults. This feature can be included in the problem formulation as follows:

$$P_i = \begin{cases} P_i^{\min} \leq P_i \leq P_{i,1}^L \\ P_{i,k-1}^U \leq P_i \leq P_{i,k}^L, k = 2, 3, \dots, n_i \\ P_{i,n_i}^U \leq P_i \leq P_i^{\max} \end{cases} \quad (23)$$

where  $n_i$  is the number of prohibited zones and  $k$  is the index of prohibited zones in unit  $i$ .  $P_{i,k}^L$  and  $P_{i,k}^U$  are the lower and upper limits, respectively, of the  $k_{th}$  prohibited zone in the  $i_{th}$  generator.

### 3.4. RAMP-RATE Limits:

The operating range of the generating units is restricted by their ramp-rate limits, which force the generators to operate continuously between two adjacent periods. The inequality constraints imposed by these ramp rate limits are as follows:

$$\max(P_{gi}^{\min}, P_i^0 - DR_i) \leq P_{gi} \leq \min(P_{gi}^{\max}, P_i^0 + UR_i)$$

where  $P_i^0$  is the power generation of the  $i_{th}$  unit in the previous hour and  $DR_i$ ,  $UR_i$ , are the decreasing and increasing ramp-rate limits, respectively, of the  $i_{th}$  unit.

### 3.5. GUPFC control variable limits:

The following control variable limits are considered:

$$r_{iq}^{\min} < r_{iq} < r_{iq}^{\max}; \forall q = j, k \quad (24)$$

$$Y_{iq}^{\min} < Y_{iq} < Y_{iq}^{\max}; \forall q = j, k \quad (25)$$

$$B_{se,iq}^{\min} < B_{se,iq} < B_{se}^{\max}; \forall q = j, k \quad (26)$$

## 4. OBJECTIVE FORMULATION

In this section, we formulate the common objectives for a multi-area power system.

### 4.1 Multi-area multi-fuel generation cost (mamfc)

We modify the conventional single-area economic dispatch problem by combining the costs of reactive power generated by the generators  $C(Q_{gi})$ , shunt compensators  $C(Q_{shi})$ , and total transmission losses  $C(TPL)$ , along with the cost of active power generated by the generators  $C(P_{gi})$  and the investment cost of the GUPFC ( $IC_{GUPFC}$ ). This function can be formulated as

$$J_{Cost} = C(P_{gi}) + C(Q_{gi}) + C(Q_{sh_i}) + C(TPL) + IC_{GUPFC} \quad (27)$$

The sub functions can be formulated as follows:

#### 4.1.1 Multi-area multi-fuel nonconvex cost of active power

In practice, generating stations are supplied with different types of fuels (coal, fossil fuel, oil and gas, etc.) to generate electrical power. A new objective function can be expressed as

$$C(P_{gi}) = \sum_1^{k=NA} \left( \sum_1^{i=NG} F_{ki}(P_{ki}) \right) \quad (28)$$

In this equation,

$$F_i(P_i) = \begin{cases} a_{i1}P_i^2 + b_{i1}P_i + c_{i1} + |e_{i1} \\ \times \sin(f_{i1}(P_i^{\min} - P_i)) \Big|; P_i^{\min} \leq P_i \leq P_i^1 \\ \vdots \\ \dots \\ a_{ij}P_i^2 + b_{ij}P_i + c_{ij} + |e_{ij} \\ \times \sin(f_{ij}(P_i^{\min} - P_i)) \Big|; P_i^{j-1} \leq P_i \leq P_i^{\max} \end{cases} \quad (29)$$

where  $a_{ij}, b_{ij}, c_{ij}, e_{ij}, f_{ij}$  are the active power cost coefficients of the  $i_{th}$  unit with valve-point effects for fuel type  $j$ , and NA is the number of areas. The cost coefficients for the generators in the multi-area system are given in Table 6.

#### 4.1.2 Multi-area multi-fuel non-convex cost of reactive power

A careful study of the literature reveals that generators active and reactive cost curves have similar characteristics. However, the cost of reactive power is less than that of active power. A new objective function for the multi-area multi-fuel non-convex reactive power cost can be expressed as

$$C(Q_{gi}) = \sum_1^{k=NA} \left( \sum_1^{i=NG} F_{ki}(Q_{ki}) \right) \quad (30)$$

$$c(Q_i) = \begin{cases} a_{ir1}Q_i^2 + b_{ir1}P_i + c_{ir1} + |e_{i1} \\ \times \sin(f_{ir1}(P_i^{\min} - P_i)) \Big|; Q_i^{\min} \leq Q_i \leq Q_i^1 \\ \vdots \\ \dots \\ a_{irj}P_i^2 + b_{irj}P_i + c_{irj} + |e_{ij} \\ \times \sin(f_{irj}(Q_i^{\min} - Q_i)) \Big|; Q_i^{j-1} \leq Q_i \leq Q_i^{\max} \end{cases} \quad (31)$$

where  $a_{irj}, b_{irj}, c_{irj}, e_{ij}, f_{irj}$  are the reactive power cost coefficients of the  $i_{th}$  unit with valve-point effects for fuel type  $j$ . The reactive cost coefficients for the generators in the multi-area system can be obtained by dividing the active power cost coefficients by 10.

#### 4.1.3. Cost of capacitors reactive power

The reactive power injected by the shunt capacitors affects the bus voltage at which it is connected. These capacitors have lower maintenance costs. Hence, the cost of the reactive power should be calculated based on the capital investment costs [54,55]

$$\sum_1^{k=NA} \left( \sum_1^{i=nc} C_{sh_i} \right) = \frac{\text{Investment cost}}{\text{Operating hours}} \quad (32)$$

#### 4.1.4 . Cost of transmission power loss

The system voltage profile and system active power losses can be modified by controlling the reactive power through transmission lines. Generally, the system losses are compensated by slack generators. The cost of active power loss in the system can be expressed as [57].

$$C(TPL) = \lambda_{\text{loss}} \times TPL \quad (33)$$

where  $\lambda_{\text{loss}} = 20$  \$/MW-h is the market energy price and TPL is the total transmission power loss (in MW), as determined by Eq. 33.

#### 4.2. Multi-area multi-fuel emission objective (mamfe)

The emission objective for multi-area multi-fuel generating units can be defined as

$$J_{\text{Emission}} = \sum_1^{k=NA} \left( \sum_1^{i=NG} E_{ki}(P_{ki}) \right) \quad (34)$$

$$E_i(P_i) = \begin{cases} \gamma_{i1} P_i^2 + \beta_{i1} P_i + \alpha_{i1} + \zeta_{i1} \exp^{\lambda_{i1} P_i}; \\ P_i^{\min} \leq P_i \leq P_i^1 \\ \vdots \\ \dots \\ \gamma_{ij} P_i^2 + \beta_{ij} P_i + \alpha_{ij} + \zeta_{ij} \exp^{\lambda_{ij} P_i}; \\ P_i^{j-1} \leq P_i \leq P_i^{\max} \end{cases} \quad (35)$$

where  $\gamma_{ij}, \beta_{ij}, \alpha_{ij}, \zeta_{ij}, \lambda_{ij}$  are the emission coefficients of the  $i_{th}$  unit for fuel type  $j$ . The emission coefficients for the generators of the multi-area system are given in Table 7.

### 4.3. Total transmission power loss (tpl)

In a power system, the active power loss should be minimized to enhance power delivery performance. The active power loss for a given multi-area system can be calculated using

$$J_{\text{TPL}} = \sum_1^{k=nl} g_k \left[ V_i^2 + V_j^2 - 2V_i V_j \cos(\delta_i - \delta_j) \right] \quad (36)$$

## 5. OVER VIEW OF BAT ALGORITHM

BAT algorithm is an optimization algorithm motivated by the echolocation behaviour of natural bats in finding their foods. It is introduced by Yang and is used for solving many real world optimization problems. Each virtual bat in the initial population employs a homologous manner by doing echolocation for updating its position. Bat echolocation is a perceptual system in which a series of loud ultrasound waves are released to produce echoes. These waves are returned with delays and various sound levels which make bats to discover a specific prey as shown in Fig 3. Some guidelines are studied to enhance the structure of BAT algorithm and use the echolocation nature of bats[61,63].

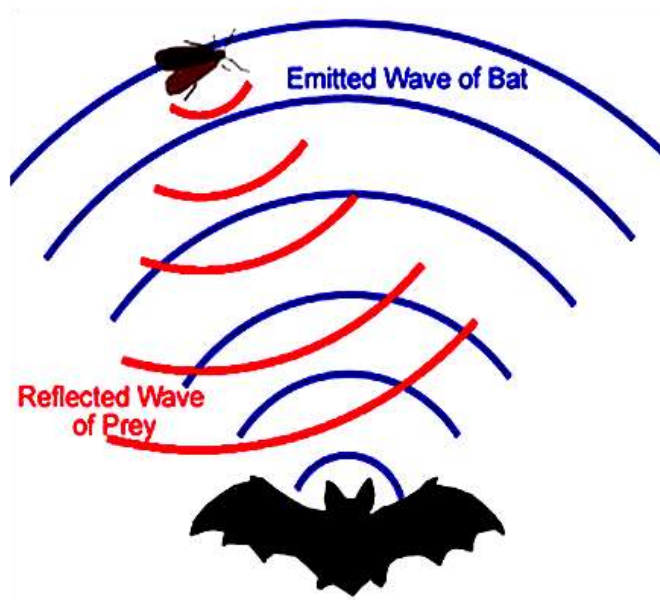


Fig .3.Echolocation behaviour of bats.

1. Each bats identify the distance between the prey and background barriers using echolocation.
2. Bats fly randomly with velocity  $v_i$  at position  $x_i$  with a fixed frequency  $f_{\min}$  (or Wavelength  $\lambda$ ), varying wavelength  $\lambda$  (or frequency  $f$ ) and loudness  $A_0$  to search for prey. They can naturally adopt the wavelength (or frequency) of their emitted pulses and adjust the rate of pulse emission  $r \in [0, 1]$ , depending on the closeness of their prey;
3. Although the loudness of the bats can be modified in many ways, we consider that the loudness varies from a large (positive)  $A_0$  to a minimum value  $A_{\min}$  according to the problem taken.



### 5.1. Initialization of bat population

Population initialization of bats randomly in between the lower and the upper boundary can be achieved by the equation.

$$x_{ij} = x_{\min j} + \text{rand}(0,1) * (x_{\max j} - x_{\min j}) \quad (37)$$

where  $i=1, 2, \dots, n$ ,  $j=1, 2, \dots, d$ ,  $x_{\min j}$  and  $x_{\max j}$  are lower and upper boundaries for dimension  $j$  respectively.

### 5.2. Update process of frequency, velocity and solution

The step size of the solution is controlled with the frequency factor in BA. this frequency factor is generated randomly in between the minimum and maximum frequency [ $f_{\min}$ ,  $f_{\max}$ ]. Velocity of a solution is proportional to frequency and new solution depends on its new velocity and it is represented as.

$$f_i = f_{\min} + (f_{\max} - f_{\min}) \beta \quad (38)$$

$$v_i^t = v_i^{t-1} + (x_i^t - x^*) f_i \quad (39)$$

$$x_i^t = x_i^{t-1} + v_i^t \quad (40)$$

Where  $\beta \in [0, 1]$  indicates randomly generated number,  $x^*$  represents current global best solutions. For local search part of algorithm (exploitation) one solution is selected among the selected best solutions and random walk is applied.

$$x_{\text{new}} = x_{\text{old}} + A^t \quad (41)$$

Where  $A^t$ , is average loudness of all bats,  $\epsilon \in [0, 1]$  is random number and represents direction and intensity of random-walk.

### 5.3. Update process of loudness and pulse emission rate

As iteration increases, the loudness and pulse emission must be updated because when the bat gets closer to its prey then their loudness  $A$  usually decreases and pulse emission rate also increases, the updating equation for loudness and pulse emission is given by

$$A_i^{t+1} = \alpha A_i^t \quad (42)$$

$$r_i^{t+1} = r_i^0 \left[ 1 - e^{(-\gamma t)} \right] \quad (43)$$

where  $\alpha$  and  $\gamma$  are constants.  $r_i^0$  and  $A_i$  are factors which consist of random values and  $A_i^0$  can typically be [1, 2], while  $r_i^0$  can typically be [0,1].

### 5.4 Pseudo code of ba

- 1) Objective function:  $f(x)$ ,  $x=(x_1 \dots x_d)^t$
- 2) Initialize bat population  $x_i$  and velocity  $v_i$   $i=1, 2 \dots n$
- 3) Define pulse frequency  $f_i$  at  $x_i$
- 4) Initialize pulse rate  $r_i$  and loudness  $A_i$
- 5) While ( $t <$  maximum number of iterations)
- 6) Generate new solutions by adjusting frequency, and updating velocities and location/solutions.
- 7)  $F$  ( $\text{rand} > r_i$ )
- 8) Select a solution among the best solutions
- 9) Generate a local solution around the selected best solution
- 10) End if
- 11) If ( $\text{rand} < A_i$  and  $f(x_i) < f(x^*)$ )
- 12) Accept new solutions
- 13) Increase  $r_i$ , reduce  $A_i$
- 14) End if
- 15) Ranks the bats and find current best  $x^*$
- 16) End while
- 17) Display results.

### 5.5. Improved bat algorithm (iba)

Bat Algorithm is an efficient algorithm at exploitation but has some insufficiency at exploration [63], thus it can easily get trapped in local minimum on most of the multimodal test functions. In order to overcome this problem of standard BA, some modifications are made in the update process of frequency to improve exploration and exploitation capability of BA.

Normally, in bat algorithm the frequency is randomly generated in between the minimum and maximum value, this frequency will have same effect to all dimensions of solution. In order to adopt the effect of change in dimensions on solutions a dynamic frequency varying concept is assigned in this improved bat algorithm.

$$\text{diff}_j = \sqrt{(x_{ij} - x_j^*)^2} \quad (44)$$

$$\text{range} = \max(\text{diff}) - \min(\text{diff}) \quad (45)$$

$$f_j = f_{\min} + \frac{\sqrt{(\min(\text{diff}) - (\text{diff}_j))^2}}{\text{range}} * (f_{\max} - f_{\min}) \quad (46)$$

The distances between  $i_{th}$  solution and global best solution are calculated first then the frequency updating are assigned according to Eq. (45), so the frequency variation is depend on difference in distances as per the Eq. (44). By varying the Frequency the step size of the solutions also varied. Thus, dimensions which are closer to global optimum point do not steer for irrelevant regions. Instead, they locally search around global optimum point. Velocity formulation Eq. (47) must be updated as follows

$$v_{ij}^t = v_{ij}^{t-1} + (x_{ij}^t - x_{ij}^*) f_j \quad (47)$$

### 5.6. Pseudo code for improved bat algorithm

- 1). Initialize the population of  $n$  bats randomly and evaluate the objective function for all bats.
- 2). Initialize temporary best solution among the solutions.
- 3). Define frequency as per the Eq. (44 - 46).
- 4). Define loudness  $A_i$  and the initial velocities  $v_i$  ( $i= 1, 2, \dots, N$ ); Set pulse rate  $r_i$ .
- 5). While ( $t < \text{maximum number of iterations}$ )
- 6). Evaluate objective function for generating new solutions by varying the frequency and update velocity Eq. (46).
- 7). If ( $\text{rand} > r_i$ )
- 8). Select a solution among the best solutions.
- 9). Generate a local solution around the selected best solution.
- 10). End if
- 11). If ( $\text{rand} < A_i$  and  $f(x_i) < f(x^*)$ )
- 12). Accept new solutions
- 13). Increase  $r_i$ , reduce  $A_i$
- 14). End if
- 15). Ranks the bats and find current best  $x^*$
- 16). End while
- 17). Display results.

### 5.7 pseudo code for the application of multi area economic dispatch with gupfc

1. Initialize the system data, algorithm data, GUPFC data and set iteration=0;
2. Initialize the population for the control variables and for the algorithm (ie velocity and frequency for the bats)
3. Update the system data (i.e jacobian matrix etc...) and the control variables for the GUPFC and solve the Newton Raphson load flow with GUPFC.
4. Convert the constrained multi area opf problem into unconstrained multi area opf problem using penalty approach.
5. Evaluate the objective function and initialize the local best.
6. select the global best solution.
7. If iteration is equal to the iteration maximum value print the best solution and stop, otherwise continue to next step.
8. Update the velocity and frequency of all the bats and update the position of control variables.
9. Check for the constraint violation (ie. POZ, Generation lower and upper limit, ramp rate limit, multi fuel option) if any violation occur goto step 8 , otherwise continue.
10. Increase the iteration counter and goto step 3.

## 6. RESULTS AND ANALYSIS

To authenticate the pertinency of the suggested approach, An IEEE-30 bus system with 41 transmission lines as the major area [58–60]. A simplified representation of the multi-area system and its three subareas is shown in Fig. 4. The corresponding data are given in Tables 8 and 9. There are a total of 24 control variables in this system, including active power generations and voltage levels for nine generators, four tap settings for tap-changing transformers, and two shunt VAr sources.

To resolve the impact of the GUPFC on the prescribed objectives, each of the accompanying cases is advanced with and without the GUPFC, and the relating results are organized for comparison.

Cases 1, 2, and 3 relate to the results for the individual MAMFC (Multi Area Multi Fuel Cost), MAMFE (Multi Area Multi Fuel Emission), and TPL (Transmission Power Loss) objectives. Initially, the severity function given in Eq. 8

is optimized. The optimal location for the GUPFC is identified by performing the procedure described in Sect. 2.2. The results of contingency analysis for this system are given in Table.1 and the MVA flow on the transmission lines during the contingency is shown in fig.5 To keep up continuity in supplying and receiving power, no contingency analysis is performed on lines between buses 9–11, 12–13, 25–26, and A2–20.

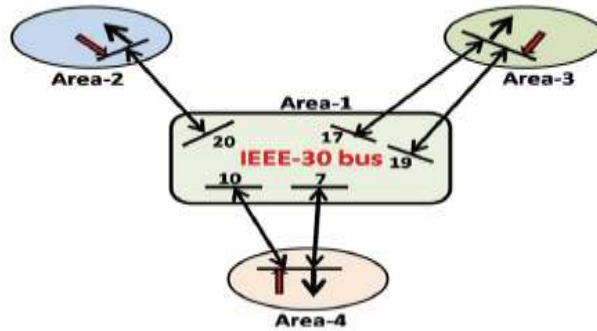


Fig.4 .Test System Considered

Hence, the contingency is performed only for 42 transmission lines out of 46 .From the contingency result it is clear that line 5 is the most critical. i.e., between buses 2 and 5.If this line is removed from the system, lines 1–2, 2–4, 2–6, 4–6, 5–7, and 6–8 become overloaded.

Table.1.Contingency result

Line no	5
Outage line	2–5
Overloaded lines	(1–2) (165.812/130) (2–4) (80.671/65) (2–6) (112.324/65) (4–6) (115.369/90) (5–7) (102.845/70) (6–8) (37.621/32)
NOLL	6
Voltage violated buses	–
NVVB	0
PI	6
Rank	1

Therefore, line 5 is assigned as rank 1. Following the rules given in Sect. 2, there are 23 possible GUPFC installation locations (excluding tie-lines).The severity function is estimated at each location, and the five locations with the lowest severity values are tabulated in Table 2 for rank-1 contingency.

Table.2.Severity function value

sLocation No.	GUPFC location			Severity function value
	Sending end bus	Receiving end bus		
1	12	14	15	1.4981
2	12	14	16	1.5748
3	15	12	23	1.5986

From this table, it is clear that the first location is the best position for the GUPFC, because it gives the lowest severity function value. The following analysis assumes the device is placed in this location.

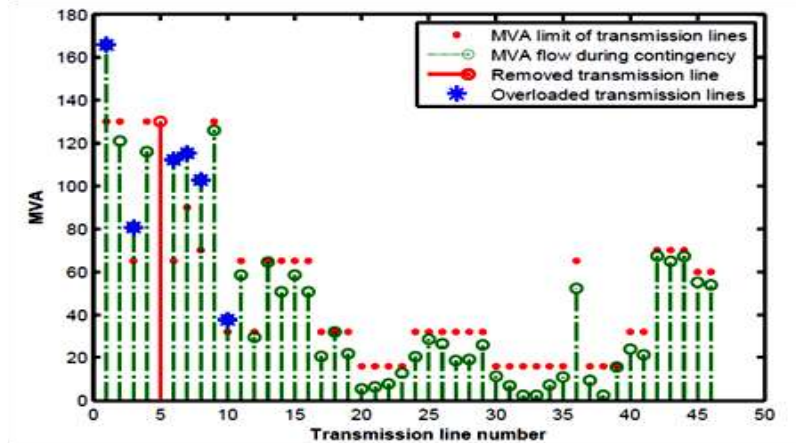


Fig.5 .Plot for contingency analysis

### CASE-1 (MAMFC)

The results from the proposed method for Cases 1 is tabulated in Table 3. From this table, it is clear that while minimizing fuel cost other objectives such as emission cost and the transmission cost increases. The total generation cost includes the costs of active, reactive, and shunt capacitor power, as well as transmission losses, with and without the GUPFC.

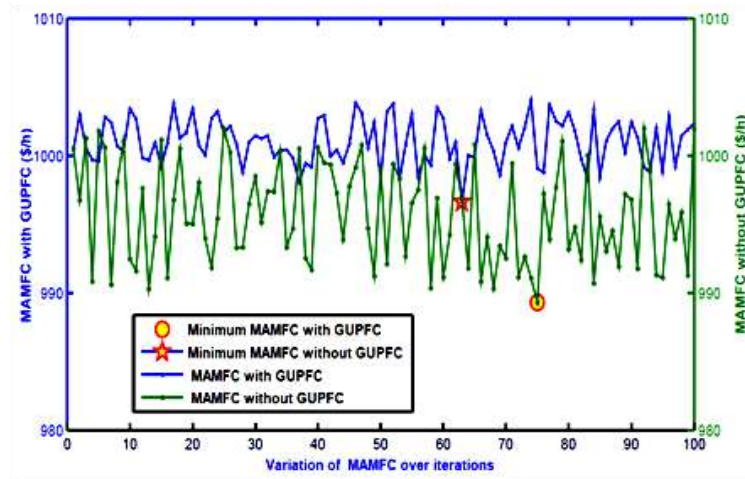


Fig.5 .Variation of MAMFC over iterations.

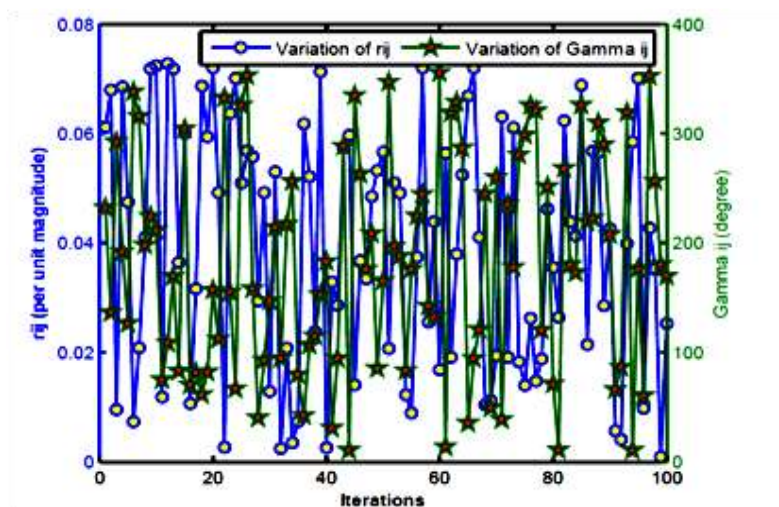


Fig.6 . Parameter variation of series converter I.

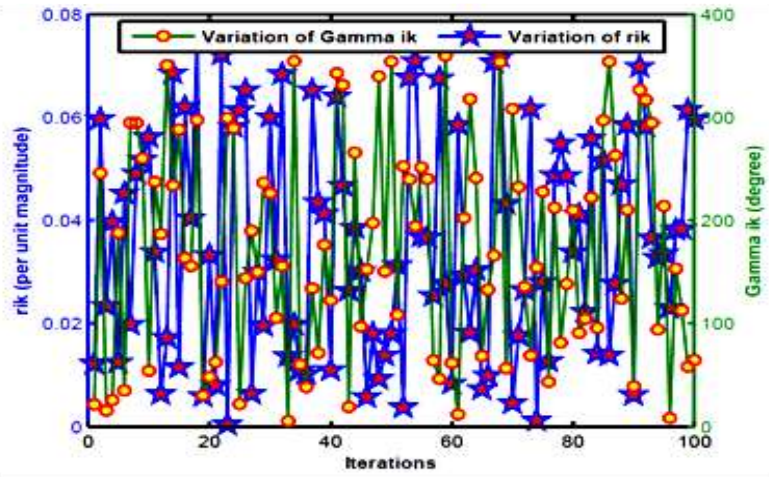


Fig.7 . Parameter variation of series converter II.

The use of this generalized UPFC results in a net cost saving of 7.3393 \$/h in Case 1 and the Fig6 and Fig7 shows the parameter variation of converters over the iteration in GUPFC.

Table.3.MAMFC

Control variables	Case-1 MAMFC		Without GUPFC	With GUPFC
<b>Real power generation (mw)</b>	<b>NSUDTPSO</b>		<b>proposed IBA</b>	
PA1-1	116.8162	108.0481	117.2606	108.4925
PA1-2	50	49.9375	50.4444	50.3819
PA1-5	20.3937	36	20.8381	32.4444
PA1-8	22.0162	17.7486	18.4606	18.1930
PA1-11	16.3615	19.6651	16.8059	20.1095
PA1-13	20.2252	14.3978	20.6696	14.8422
PA2	49.9304	48.0608	50.3748	48.5052
PA3	53.8129	54.5757	54.2573	55.0201
PA4	54.5734	54.8288	55.0178	55.2732
<b>Gen voltage</b>				
VA1-1	1.05	1.0408	1.491	1.0416
VA1-2	0.9798	1.0343	0.9237	1.0369
VA1-5	1.0083	0.9939	1.0173	0.9112
VA1-8	1.05	1.0014	1.05	1.0355
VA1-11	1.0152	0.9927	1.0185	0.9632
VA1-13	1.0229	1.0197	1.0154	1.0283
VA2	1.0309	1.0241	1.0290	1.0145
VA3	1.0382	1.024	1.0351	1.0329
VA4	0.9925	1.0132	0.9933	1.0257
<b>REACTIVE POWER</b>				
QA1-1	8.2354	-12.652	8.6798	-12.2076
QA1-2	- 20	38.5047	-19.5556	38.9491
QA1-5	22.8486	11.3339	23.2930	11.7783
QA1-8	60	14.1117	56.4444	14.5561
QA1-11	- 3.4695	-2.9315	-3.0251	-2.4871
QA1-13	- 5.8455	11.585	-5.4011	12.0294
QA2	18.5145	24.1708	18.9589	24.6152
QA3	30.4474	26.9189	30.8918	27.3633
QA4	10.6562	19.1832	11.1006	19.6276
Tap 6-9, p.u.	1.0158	1.0399	1.0145	1.0254
Tap 6-10, p.u.	1.0419	0.9303	1.0312	0.965

Tap 4-12, p.u.	0.9613	1.0316	0.9452	1.0254
Tap 28-27, p.u.	1.004	0.973	1.002	0.965
Qc 10, p.u.	25.2545	20.7762	24.9311	19.3371
Qc 24, p.u.	21.3987	15.3358	19.9664	16.8551
<b>GUPFC</b>				
$r_{ij}$ , p.u.	-	0.017	-	0.014
$r_{ik}$ , p.u.	-	0.0396	-	0.028
$\gamma_{ij}$ , deg.	-	282.5022	-	298.3258
$\gamma_{ik}$ , deg.	-	262.3598	-	227.8861
$X_{se,ij}$ , p.u.	-	0.0086	-	0.0079
$X_{se,ik}$ , p.u.	-	0.0101	-	0.0141
Qsh, p.u.	-	0.0383	-	0.0392
Inv. Cost, \$/h	-	0.1563	-	0.1556
Total PCost, \$/h	829.4125	858.1611	824.5784	847.8391
Total QCost, \$/h	54.393	41.0181	52.0419	38.667
TPL cost, \$/h	118.5902	101.1262	118.57	101.562
Total Qccost\$/h.	1.7038	1.3188	1.449	1.2279
<b>MAMFC, \$/h</b>	<b>1,004.099</b>	<b>1,001.781</b>	<b>996.6393</b>	<b>989.3</b>
MAMFE, ton/h	0.2629	0.256	0.831	0.293
TPL, MW	5.9295	5.0563	5.8981	5.0781
Total Pgen, MW	404.1295	403.2624	404.1291	403.2620
Total Qgen,	121.387	130.2245	121.388	134.2243

#### CASE-2 (MAMFE)

In this case the use of generalized UPFC results in a net cost saving of 0.0021 ton/h emission reduction and the Fig9 and Fig10 shows the parameter variation of converters over the iteration in GUPFC for MAMFE case.

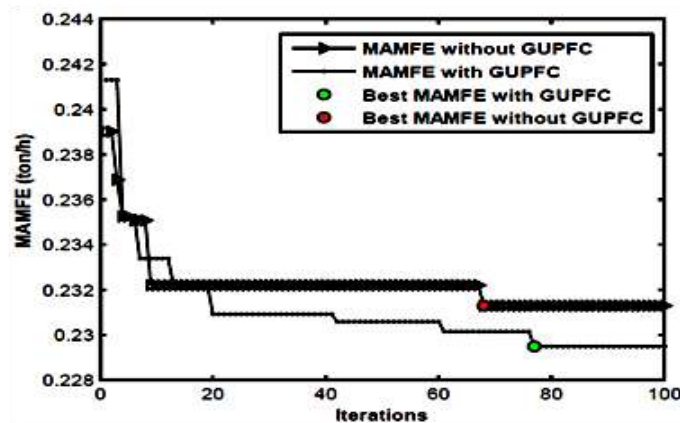


Fig.8 . Convergence characteristics of MAMFC

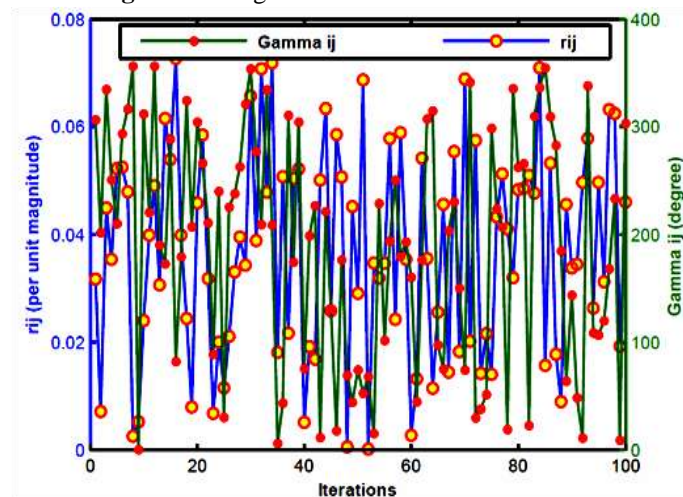


Fig.9 . Parameter variation of series converter I.

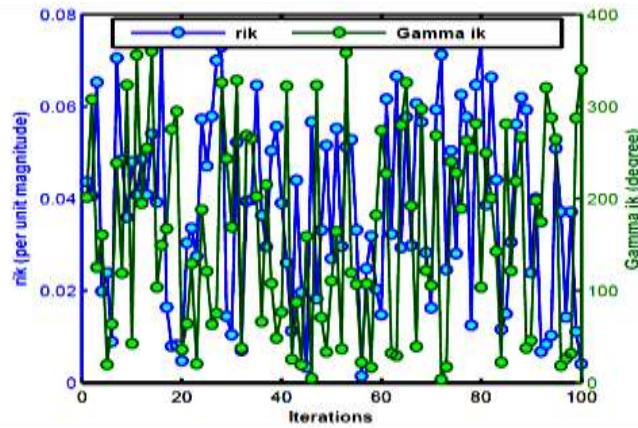


Fig.10 . Parameter variation of series converter II.

Table.4.MAMFE

Control variables	Case-2 MAMFE			
	NSUDTPSO		proposed IBA	
	Without GUPFC	With GUPFC	Without GUPFC	With GUPFC
<b>Real power generation (mw)</b>				
PA1-1	70.2355	60.0443	70.6799	60.4887
PA1-2	50	49.9893	48.4528	48.4337
PA1-5	36	48.8825	36.7428	49.3269
PA1-8	25	25	25.2534	25.2147
PA1-11	28	25	28.5289	25.5216
PA1-13	35	34.7896	35.3368	35.2340
PA2	49.9717	49.4848	50.4161	49.9292
PA3	54.3799	54.6811	52.8243	53.1255
PA4	54.9946	54.7793	55.4390	55.2237
<b>Gen voltage</b>				
VA1-1	0.9704	1.0137	0.9613	1.0211
VA1-2	0.9849	1.05	0.9729	1.05
VA1-5	0.9756	1.0195	0.9856	1.0185
VA1-8	1.0326	0.9777	1.0352	0.9693
VA1-11	1.0486	0.9829	1.0483	0.9956
VA1-13	1.0108	0.9885	1.0128	0.99
VA2	1.0399	1.0183	1.0358	1.0174
VA3	1.0243	0.998	1.0217	0.986
VA4	0.9812	1.0273	0.9963	1.0269
<b>REACTIVE POWER</b>				
QA1-1	- 63.9288	-59.6079	-63.4844	-59.1635
QA1-2	7.704	100	8.1484	100.4444
QA1-5	20.0839	36.9734	20.5283	37.4178
QA1-8	60	-15	60.0000	-14.5556
QA1-11	9.892	- 4.4834	10.3364	-4.0390
QA1-13	19.0403	- 1.1945	19.4847	-0.7501
QA2	34.724	35.9824	35.1684	36.4268
QA3	24.1159	11.65	24.5603	12.0944
QA4	12.1964	24.7774	12.6408	25.2218
Tap 6-9, p.u.	0.9808	1.0004	0.9654	1.0002

Tap 6-10, p.u.	1.0279	1.0106	1.0158	1.0121
Tap 4-12, p.u.	1.0964	0.9893	1.0856	0.9785
Tap 28-27, p.u.	1.0411	0.979	1.0415	0.965
Qc 10, p.u.	22.8353	20.9367	21.4786	20.3856
Qc 24, p.u.	24.3935	13.4243	25.3935	14.3845
<b>GUPFC CONTROL PARAMETERS</b>				
$r_{ij}$ , p.u.	–	0.0429	–	0.0431
$r_{ik}$ , p.u.	–	0.0131	–	0.0158
$\gamma_{ij}$ , deg.	–	233.4719	–	246.6582
$\gamma_{ik}$ , deg.	–	299.9634	–	282.7451
$X_{se,ij}$ , p.u.	–	0.0143	–	0.0156
$X_{se,ik}$ , p.u.	–	0.0069	–	0.0072
Qsh, p.u.	–	0.0373	–	0.0356
Inv. Cost, \$/h	–	0.0752	–	0.0748
Total PCost, \$/h	948.5742	1001.69	949.9898	1002.209
Total QCost, \$/h	64.4896	63.703	62.4627	63.615
TPL cost, \$/h	107.6334	88.8957	105.472	90.784
Total Qccost, \$/h.	1.7248	1.2549	1.6216	1.2211
MAMFC, \$/h	1,122.422	1,155.58	1119.5461	1157.829
MAMFE, ton/h	<b>0.2332</b>	<b>0.2311</b>	<b>0.2316</b>	<b>0.2295</b>
TPL, MW	5.3817	4.4448	5.2736	4.5392
Total Pgen, MW	403.5817	402.6509	403.5813	402.6505
Total QgenMVar	123.8277	129.0975	127.3829	133.0970

### CASE-3 (TPL)

In this case the use of generalized UPFC results in a net cost saving of 0.2387 MW loss reduction and the Fig12 and Fig13 shows the parameter variation of converters over the iteration in GUPFC for MAMFE case.

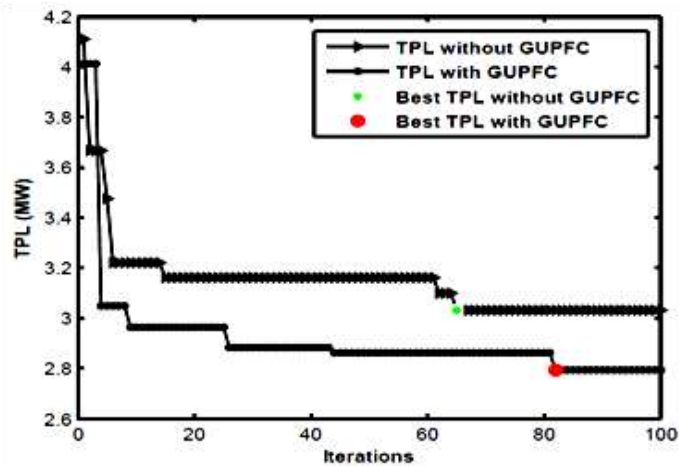


Fig.11 . Convergence characteristics of MAMFC



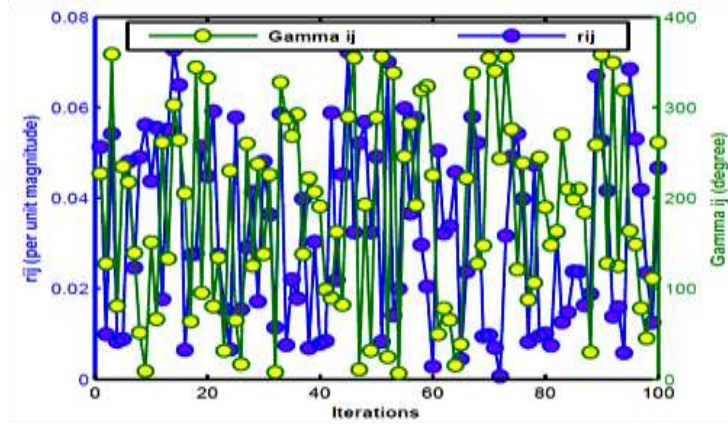


Fig.12 . Parameter variation of series converter I.

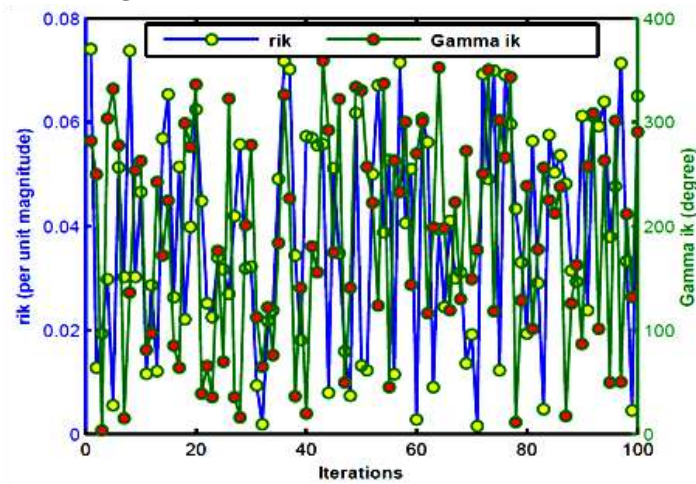


Fig.13 . Parameter variation of series converter II.

Table.5.TPL

Control variables	Case-3 TPL			
	NSUDT PSO		proposed IBA	
	Without GUPFC	With GUPFC	Without GUPFC	With GUPFC
Real Power generation (mw)				
PA1-1	70.4956	70.3571	70.0512	69.913
PA1-2	32.9098	28.5244	32.4654	28.080
PA1-5	35.6281	33.7861	35.1837	33.342
PA1-8	20.4223	25	19.9779	24.556
PA1-11	23.032	28	22.5876	27.558
PA1-13	30	31.3095	29.5556	30.862
PA2	49.2369	50	48.7925	49.553
PA3	64.859	57.7838	66.4146	59.334
PA4	75.1625	76.7018	76.7181	78.258
Gen voltage				
VA1-1	1.0346	1.0425	1.0254	1.0316
VA1-2	1.0261	1.0293	1.0214	1.0242
VA1-5	0.9925	1.0156	0.9814	1.0148
VA1-8	0.9986	1.0281	0.9712	1.0145
VA1-11	1.002	1.0001	1.011	1.025
VA1-13	1.05	1.0251	1.045	1.017
VA2	1.05	1.0238	1.05	1.0247

VA3	1.05	1.0241	1.0286	1.0194
VA4	1.0438	1.0421	1.0395	1.0457
<b>REACTIVE POWER</b>				
QA1-1	- 2.5238	5.4275	-2.9682	4.9831
QA1-2	22.8286	- 4.4622	22.3842	4.9066
QA1-5	11.7493	27.0817	11.3049	26.637
QA1-8	- 0.4583	39.1501	-0.9027	38.706
QA1-11	- 5.7568	- 7.9829	-6.2012	8.4273
QA1-13	13.2827	10.3269	12.8383	9.8825
QA2	26.2777	20.2397	25.8333	19.796
QA3	31.5185	17.0256	31.0741	16.582
QA4	25.8964	24.8261	25.4520	24.387
Tap 6-9, p.u.	1.0198	0.998	1.0175	0.9
Tap 6-10, p.u.	0.9757	0.988	0.9652	0.956
Tap 4-12, p.u.	0.9947	0.9957	0.9862	0.9831
Tap 28-27, p.u.	1.0013	0.9908	1.0047	0.99
Qc 10, p.u.	20.7525	19.4298	20.832	20.135
Qc 24, p.u.	20.7949	12.1666	19.365	17.566
<b>GUPFC CONTROL PARAMETERS</b>				
$r_{ij}$ , p.u.	–	0.0283	–	0.0325
$r_{ik}$ , p.u.	–	0.0328	–	0.029
$\gamma_{ij}$ , deg.	–	157.084	–	163.24
$\gamma_{ik}$ , deg.	–	170.546	–	177.45
$X_{se,ij}$ , p.u.	–	0.0166	–	0.014
$X_{se,ik}$ , p.u.	–	0.0151	–	0.0149
Qsh, p.u.	–	0.077	–	0.065
Inv. Cost, \$/h	–	0.0922	–	0.095
Total PCost, \$/h	1,078.058	1,141.79	1073.42	1136.9
Total QCost, \$/h	36.476	51.6729	35.776	50.948
TPL cost, \$/h	70.9248	64.8896	60.634	55.86
Total Qccost, \$/h.	1.5173	1.1539	1.560	1.3156
MAMFC, \$/h	1,186.976	1,259.57	1173.18	1244.9
MAMFE, ton/h	0.2554	0.2543	0.2356	0.2556
TPL, MW	<b>3.0506</b>	<b>2.8875</b>	<b>3.0317</b>	<b>2.793</b>
Total Pgen, MW	401.7462	401.467	401.747	401.48
Total Qgen, MVar	122.8142	131.635	118.814	127.63

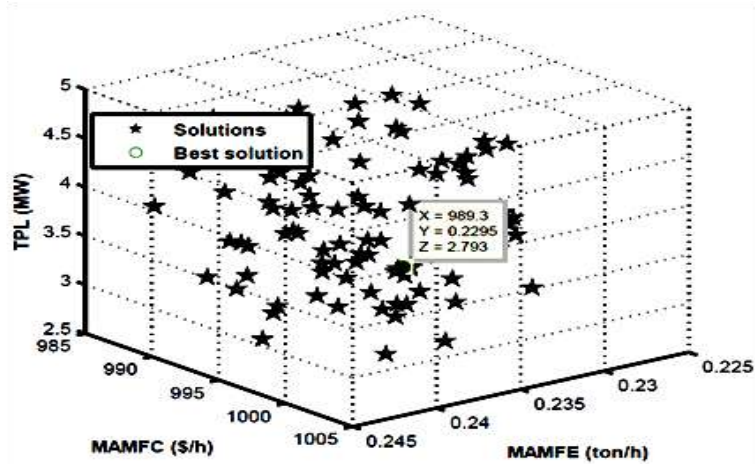


Fig.14 . Solutions with GUPFC

Figure.14 shows the evaluated solutions and the effectiveness of the proposed algorithm.

## 7. CONCLUSION

In this paper, An Improve bat algorithm was proposed to optimize the generation cost, emissions, and total power loss objectives under various practical constraints and device limits. The results obtained by this method are compared with NSUDTPSO algorithm. The comparison shows that IBA performs better than above mentioned method. The IBA has superior features including quality of solution, stable convergence characteristics and good computational efficiency for large system. Therefore, this results shows that IBA is a promising technique for solving complicated problems in power system.

## 8. REFERENCES

- [1]. Song, Y.H. and In-Keun Yu, “Dynamic load dispatch with voltage security and environmental constraints”, Electric Power System Research, Vol. 43, pp. 53-60, 1997.
- [2]. Shoults, Chang R.R., Helmick, S.K. and Grady, W.M. “A practical approach to unit commitment, economic dispatch and savings allocation for multiple-area pool operation with import / export constraints”, IEEE Transactions on Power Apparatus and Systems, Vol. 99, No. 2, pp. 625-635, 1980.
- [3]. Wang, C. and Shasidehpur, S.M. “A decomposition approach to nonlinear multi-area generation scheduling with tie-line constraints using expert systems”, IEEE Transactions on Power systems, Vol. 7, No. 4, pp. 1409-1418, 1992.
- [4]. Wang, C. and Shasidehpur, S.M. “Power generation scheduling for multi-area hydro thermal systems with tie line constraints, cascaded reservoirs and uncertain data”, IEEE Transactions on Power Systems, Vol. 8, No. 3, pp. 1333-1340, 1993.
- [5]. Streiffert, D. “Multi-area Economic Dispatch with tie-line constraints”, IEEE Transactions on Power systems, Vol. 10, No. 4, pp. 1946-1951, 1995.
- [6]. Basu, M.: Improved differential evolution for economic dispatch. *Electr. Power Energy Syst.* 63, 855–861 (2014).
- [7]. Bhattacharjee, K.; Bhattacharya, A.; Dey, S.H.N.: Oppositional real coded chemical reaction optimization for different economic dispatch problems. *Electr. Power Energy Syst.* 55, 378–391 (2014).
- [8]. Ghasemi, M.; Ghavidel, S.; Rahmani, S.; Roosta, A.; Falah, H.: A novel hybrid algorithm of imperialistic competitive algorithm and teaching learning algorithm for optimal power flow problem with non-smooth cost functions. *Eng. Appl. Artif. Intell.* 29, 54– 69 (2014).
- [9]. Christy, A.; Ajay, P.; Raj, D.V.: Adaptive biogeography based predator-prey optimization technique for optimal power flow. *Electr. Power Energy Syst.* 62, 344–352 (2014).
- [10]. Babu, A.V.N.; Ramana, T.; Sivangaraju, S.: Analysis of optimal power flow problem based on two stage initialization algorithm. *Electr. Power Energy Syst.* 55, 91–99 (2014).
- [11]. Mandal, B.; Roy, P.K.; Mandal, S.: Economic load dispatch using krill herd algorithm. *Electr. Power Energy Syst.* 57, 1–10 (2014).
- [12]. vijayaraj.S and R.K.Santhi .: Multi-area economic dispatch using Improved bat algorithm. *International Journal of Applied Engineering Research* . Volume 10, pp 40139-40147, (2015).
- [13]. Niu, Q.; Zhang, H.; Wang, X.; Irwin, G.W.: A hybrid search with arithmetic crossover operation for economic dispatch. *Electr. Power Energy Syst.* 62, 237–257 (2014)
- [14]. dos Santos Coelho, L.; Bora, T.C.; Mariani, V.C.: Differential evolution based on truncated Levy-type flights and population diversity measure to solve economic load dispatch problems. *Electr. Power Energy Syst.* 57, 178–188 (2014).

- [15]. Abido, M.A.; Al-Ali, N.A.: Multi-objective optimal power flow using differential evolution. Arab. J. Sci. Eng. 37(4), 991–1005 (2012)
- [16]. Coello, C.A.C.: A comprehensive survey of evolutionary based multi-objective optimization techniques. Knowl. Inf. Syst. 1(3), 269–308 (1999).
- [17]. Abido, M.A.: Environmental/economic power dispatch using multi-objective evolutionary algorithms. IEEE Trans. Power Syst. 18(4), 1529–1537 (2003).
- [18]. Andrew, K.; Haiyang, Z.: Optimization of wind turbine energy and power factor with an evolutionary computation algorithm. Energy 35(3), 1324–1332 (2010)
- [19]. Srinivas, N.; Deb, K.: Multiobjective optimization using nondominated sorting in genetic algorithms. Evol. Comput. 2(3), 221–248 (1994)
- [20]. Abido, M.A.: A novel multiobjective evolutionary algorithm for environmental/economic power dispatch. Electr. Power Syst. Res. 65, 71–81 (2003)
- [21]. Chang, C.S.; Liew, A.C.; Xu, J.X.; Wang, X.W.; Fan, B.: Dynamic security constrained multiobjective generation dispatch of longitudinally interconnected power systems using bicriterion global optimization. IEEE/PES Summer Meeting, SM 578-5 (1995)
- [22]. Streiffert, D.: Multi-area economic dispatch with tie line constraints. IEEE/PES Winter Meeting, WM 179-2 (1995)
- [23]. Romano, R.; Quintana, V.H.; Lopez, R.; Valadez, V.: Constrained economic dispatch of multi-area systems using the Dantzig–Wolfe decomposition principle. IEEE Trans. PAS 100(4), 2127–2137 (1981)
- [24]. Ouyang, Z.; Shahidehpour, S.M.: Heuristic multi-area unit commitment with economic dispatch. IEE Proc.-C 138(3), 242–252 (1991)
- [25]. Wernerus, J.; Soder, L.: Area price based multi-area economic dispatch with tie line losses and constraints, In: IEEE/KTH Stockholm Power Tech Conference, Sweden, pp. 710–715 (1995).
- [26]. Lai, L.L. and Ma, J.T. “Power flow control in FACTS using Evolutionary Programming”, IEEE Transactions on Power systems, Vol. 4, pp. 109-113, 1995.
- [27]. Prasanna, T. S. and Somasundaram, P. “OPF with FACTS devices in interconnected power systems using fuzzy stochastic algorithms,” International Journal of Power and Energy Conversion, Vol. 1, No.2, pp.279-299, 2009b.
- [28]. Abbate, L.; Trovato, M.; Becker, C.; Handschin, E.: Advanced steady-state model of UPFC for power system studies. Power Eng. Soc. Summer Meet. (IEEE) 1, 449–454 (2002).
- [29]. Esquivel, C.R.F.; Acha, E.: Unified power flow controller: a critical comparison of Newton-Raphson UPFC algorithms in power flow studies. IEE Proc. Gener. Transm. Distrib. 144(5), 437–444 (1997).
- [30]. Vural, A.M.; Tumay, M.: Mathematical modeling and analysis of a unified power flow controller: a comparison of two approaches in power flow studies and effects of UPFC location. Electr. Power Energy Syst. 29, 617–629 (2007).
- [31]. Tumay, M.; Vural, A.M.; Lo, K.L.: The effect of unified power flow controller location in power systems. Electr. Power Energy Syst. 26, 561–569 (2004)
- [32]. Nabavi, S.M.H.; Khafafi, K.; Sakhavati, A.; Nahi, S.: Optimal location and sizing of SSSC using genetic algorithm in deregulated power market. Int. J. Comput. Appl. 22(4), 37–41 (2011).
- [33]. Shaheen, H.I.; Ghamgeen, I.; Cheng, R.S.J.: Optimal location and parameter setting of UPFC for enhancing power system security based on differential evolution algorithm. Electr. Power Energy Syst. 33, 94–105 (2011).
- [34]. Schauder, C.D.; Gyugyi, L.; Lund, M.R.; et al.: Operation of the unified power flow controller (UPFC) under practical constraints. IEEE Trans. Power Deliv. 13(2), 630–639 (1998).
- [35]. Lubis, R.S.; Hadi, S.P.; Tumiran: Modeling of the Generalized Unified Power Flow Controller for Optimal Power Flow, ICEEI (IEEE), pp. 1–6 (2011)
- [36]. Zhang, X.-P.; Handschin, E.; Yao, M.M.: Modeling of the generalized unified power flow controller (GUPFC) in a nonlinear interior point OPF. IEEE Trans. Power Syst. 16(3), 367–373 (2001).
- [39]. Zhang, X.P.: Modeling of the interline power flow controller and the generalized unified power flow controller in Newton power flow. IEE Proc. Gener. Transm. Distrib. 150(3), 268–274 (2003).
- [40]. Zhang, X.P.: Robust modeling of the interline power flow controller and the generalized unified power flow controller with small impedances in power flow analysis. Electr. Eng. 89, 1–9 (2006).
- [41]. Ghadimi, N.; Afkousi-Paqaleh, A.; Emamhosseini, A.: A PSO based fuzzy long-term multi objective optimization approach for placement and parameter setting of UPFC. Arab. J. Sci. Eng. 39(4), 2953–2963 (2014).
- [42]. Azizpanah-Abarghoee, R.; Narimani, M.R.; Bahmani-Firouzi, B.; Niknam, T.: Modified shuffled frog leaping algorithm for multi-objective optimal power flow with FACTS devices. J. Intell. Fuzzy Syst. 26, 681–692 (2014).
- [43]. Nandakumar, E.; Dhanasekaran, R.: Optimal power flow with FACTS controllers using hybrid PSO. Arab. J. Sci. Eng. 39(4), 3137–3146 (2014).
- [44]. Bhattacharyya, B.; Gupta, V.K.: Fuzzy based evolutionary algorithm for reactive power optimization with FACTS devices. Electr. Power Energy Syst. 61, 39–47 (2014).
- [45]. Dandachi, N.H.; Rawlins, M.J.; Alsac, O.; Paris, M.; Stott, B.: For OPF reactive pricing studies on the NGC system. IEEE Trans. Power Syst. 11(1), 11–17 (1996).
- [46]. Wills, L.; Finney, J.; Ramon, G.: Computing the cost of unbundled services. IEEE Comput. Appl. Power Syst. 9(4), 16–21 (1996).

- [47]. Lamont, J.W.; Fu, J.: Cost analysis of reactive support. *IEEE Trans. Power Syst.* 14, 890–898 (1999).
- [48]. Paucar, V.L.; Rider, M.J.: Reactive power pricing in deregulated electrical markets using a methodology based on the theory of marginal costs. In: *Proceedings of the IEEE Large Engineering Systems Conference on Power Engineering*, pp. 7–11 (2001).
- [49]. Vigneshwaran.D.; Sivakumar.;R, Vijayaraj.S.: Flower Pollination Algorithm for Economic Dispatch problem with Prohibited zones, Ramp rate limits & Multi-fuel options, *International Journal of Advanced Research in Electrical, Electronics and Instrumentation Engineering*, Vol. 4, Issue 11, pp no 1-8 November 2015.
- [50]. Chintalapudi Venkata Suresh and Sirigiri Sivanaga Raju.: Mathematical modelling and analysis of a Generalized Unified Power Flow Controller with Device rating Methodology, *International Journal on Electrical Engineering and Informatics - Volume 7*, pp.59-78, March 2015.
- [51]. Chintalapudi V Suresh, Sirigiri Sivanagaraju.: Analysis and effect of Generalized Unified power flow controller: An optimal location strategy, *International Journal Of Innovative Research In Electrical, Electronics, Instrumentation And Control Engineering*, pp.2146-2153 Vol. 2, issue 10, october 2014.
- [52]. Saravanan, M.; Slochanal, S.M.R.; Venkatesh, P.; Abraham, J.P.S.: Application of particle swarm optimization technique for optimal FACTS devices considering cost of installation and system loadability. *Electr. Power Syst. Res.* **77**, 276–283 (2007)
- [53]. Manoharan, P.S.; Kannan, P.S.; Ramanathan, V.: A novel EP approach for multi-area economic dispatch with multiple fuel options. *Turkish J. Electr. Eng. Comput. Sci.* **17**(1), 1–19 (2009).
- [54]. Dai, Y.; Liu, X.D.; Ni, Y.X.; Wen, F.S.; Han, Z.H.; Shen, C.M.; Wu, F.F.: A cost allocation method for reactive power service based in power flow tracing. *Electr. Power Syst. Res.* 64, 59–65 (2003).
- [55]. Chung, C.Y.; Chung, T.S.; Yu, C.W.; Lin, X.J.: Cost-based reactive power pricing with voltage security consideration in restructured power systems. *Electr. Power Syst. Res.* 70, 85–91 (2004).
- [56]. Hao, S.: A reactive power management proposal for transmission operators. *IEEE Trans. Power Syst.* 18, 1374–1381 (2003).
- [57]. Sayah, S.; Zehar, K.: Modified differential evolution algorithm for optimal power flow with non-smooth cost functions. *Energy Convers. Manag.* 49, 3036–3042 (2008)
- [58]. Abido, M.A.: Optimal power flow using Tabu search algorithm. *Electr. Power Compon. Syst.* 30, 469–483 (2002)
- [59]. Arul, R.; Ravi, G.; Velsami, S.: Non-convex economic dispatch with heuristic load patterns, valve point loading effect, prohibited operating zones, ramp-rate limits, and spinning reserve constraints using harmony search algorithm. *Electr. Eng.* **95**, 53–61 (2013)
- [60]. Zhu, J.; Momoh, J.A.: Multi-area power systems economic dispatch using nonlinear convex network flow programming. *Electr. Power Syst. Res.* **59**, 13–20 (2001).
- [61]. X.-S. Yang, A New Metaheuristic Bat-Inspired Algorithm, in: *Nature Inspired Cooperative Strategies for Optimization (NISCO 2010)* (Eds. J. R. Gonzalez et al.), *Studies in Computational Intelligence*, Springer Berlin, 284, Springer, 65-74 (2010).
- [62]. Xin-She Yang, Bat algorithm: literature review and applications, *Int. J. Bio-Inspired Computation*, Vol. 5, No. 3, pp. 141–149 (2013). DOI: 10.1504/IJBIC.2013.055093
- [63]. Selim Yilmaz and Ecir U. Kucuksille. Improved Bat Algorithm on Continuous Optimization Problems. *Lecture Notes on Software Engineering*, Vol. 1, No. 3, August 2013.
- [64]. Zhang, X.-P.; Rehtanz, C.; Pal, B.; Flexible, A.C.: *Transmission Systems: Modelling and Control (Power Systems)*. Springer, Berlin (2006); ISBN: 3540306064.
- [65]. Chintalapudi V. Suresh · S. Sivanagaraju · J. Viswanatha Rao Multi-area Multi-fuel Economic–Emission Dispatch Using a Generalized Unified Power Flow Controller Under Practical Constraints, *Arab J Sci Eng* (2015) 40:531–549.

**APPENDIX A: OPF AND MULTI-AREA DATA**

In this section, data for Multi area economic dispatch are given.

**Table.6.** Fuel cost coefficients

Gen. no.	a	b	c	d	e	$P_G^{\min}$	$P_G^{\max}$
<b>PA1-1</b>	0.005	0.7	55	0.35	0.0032	50	140
	0.0075	1.05	82	0.254	0.00153	140	200
<b>PA1-2</b>	0.01	0.3	40	0.294	0.0029	20	55
	0.02	0.6	80	0.241	0.00165	55	80
<b>PA1-5</b>	0.0625	1	0	0	0	15	50
<b>PA1-8</b>	0.00834	3.25	0	0	0	10	35
<b>PA1-11</b>	0.025	3	0	0	0	10	30
<b>PA1-13</b>	0.025	3	0	0	0	12	40
<b>PA2</b>	0.005	0.7	55	0.35	0.0032	20	50
	0.0075	1.05	82	0.254	0.00153	50	100
<b>PA3</b>	0.01	0.3	40	0.294	0.0029	20	55
	0.02	0.6	80	0.241	0.00165	55	100
<b>PA4</b>	0.005	0.7	55	0.35	0.0032	25	55
	0.0075	1.05	82	0.254	0.001	55	100

**Table.7.** Emission coefficients co-efficients

Gen. no.	$\gamma$	$\beta$	$\alpha$	$\zeta$	$\lambda$	$P_G^{\min}$	$P_G^{\max}$
<b>PA1-1</b>	0.0418	-0.04144	0.02819	0.0002	1.667	50	140
	0.0501	-0.05116	0.03214	0.0002	2.645	140	200
<b>PA1-2</b>	0.04612	-0.05214	0.02121	0.0003	2.857	20	55
	0.05124	-0.04421	0.02413	0.0004	3.1233	55	80
<b>PA1-5</b>	0.04586	-0.05094	0.04258	0.000001	8	15	50
<b>PA1-8</b>	0.0338	-0.0355	0.05326	0.002	2	10	35
<b>PA1-11</b>	0.04586	-0.05094	0.04258	0.000001	8	10	30
<b>PA1-13</b>	0.05151	-0.05555	0.06131	0.000001	6.667	12	40
<b>PA2</b>	0.0418	-0.04144	0.02819	0.0002	1.667	20	50
	0.0501	-0.05116	0.03214	0.0002	2.645	50	100
<b>PA3</b>	0.04612	-0.05214	0.02121	0.0003	2.857	20	55
	0.05124	-0.04421	0.02413	0.0004	3.123	55	100
<b>PA4</b>	0.0418	-0.04144	0.02819	0.0002	1.667	25	55
	0.0501	-0.05116	0.03214	0.0002	2.645	55	100

**Table.8.** parameters of subareas

S. no.	Sub area	Active demand (MW)	Reactive demand (MVA <sub>r</sub> )
1	A2	44	21
2	A3	31.2	14
3	A4	39.6	18

**Table.9.** Tie line parameter.

S. no.	Tie-line	Resistance (p.u)	Reactance (p.u)	MVA limit
1	A2-20	0.034	0.068	70
2	A3-17	0.0192	0.0575	70
3	A3-19	0.0192	0.0575	70
4	A4-10	0.0267	0.82	60
5	A4-7	0.0267	0.82	60

**APPENDIX B: GUPFC MATHEMATICAL MODELING**

Let us define three GUPFC buses i, j, and k as shown in Fig. 15.

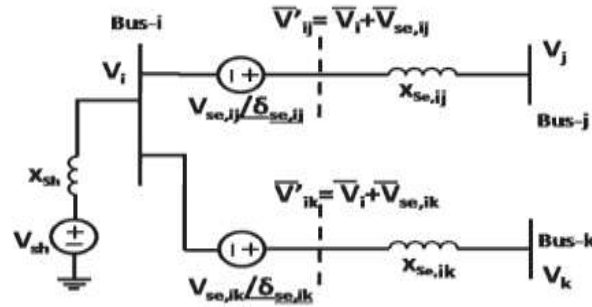


Fig. 16. Voltage source model of GUPFC

$$\bar{V}_{se_{iq}} = r_{iq} V_i e^{j(\delta_i + \gamma_{iq})}; \forall q = j, k \quad (48)$$

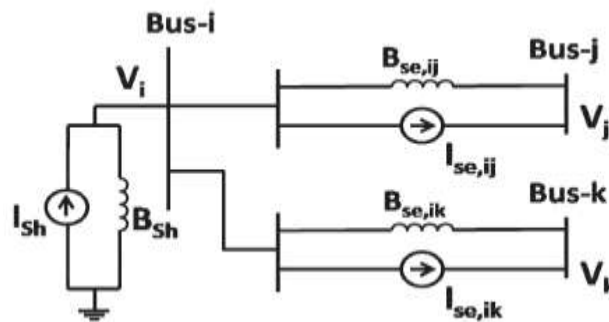


Fig. 17. Equivalent current source model of GUPFC

The voltages behind the series reactances can be calculated as

$$\bar{V}_{ij} = \bar{V}_i + \bar{V}_{se_{ij}} \text{ and } \bar{V}_{se_{ik}} = \bar{V}_i + \bar{V}_{se_{ik}} \quad (49)$$

The GUPFC power injection model can be developed using the following two models.

**B.1 SERIES CONNECTED VOLTAGE SOURCE MODEL**

According to Norton's theorem, the series-connected voltage sources can be modeled as equivalent current sources in parallel with corresponding susceptance, as shown in Fig. 17, where

$$B_{se_{iq}} = \frac{1}{X_{se_{iq}}}; \forall q = j, k \quad (50)$$

for the series transformer equivalent reactance X<sub>se</sub>. The amount of current flowing from the source is

$$\bar{I}_{se_{iq}} = -j B_{se_{iq}} \bar{V}_{se_{iq}}; \forall q = j, k \quad (51)$$

Substituting Eq. 48 into Eq. 51, we obtain

$$\left( \bar{I}_{se_{iq}} \right)^* = r_{iq} V_i B_{se_{iq}} e^{-j(90^\circ + \delta_i + \gamma_{iq})}; \forall q = j, k \quad (52)$$

Finally, this current source can be modeled by injecting equivalent power at the GUPFC connected buses. The injection powers can be expressed as

$$\bar{S}_{i_{se}} = -\bar{V}_i \sum_{q=j,k} \left( \bar{I}_{se_{iq}} \right)^* \quad (53)$$

$$\bar{S}_{p_{se}} = \bar{V}_p \left( \bar{I}_{se_{iq}} \right)^*; \forall p = j, k \quad (54)$$

Substituting Eq. 51 into Eqs. 52 and 53, the individual power injections can be derived as

$$P_{i_{se}} = -V_i^2 \left[ \sum_{q=j,k} r_{iq} B_{se_{iq}} \sin \sin \gamma_{iq} \right] \quad (55)$$

$$Q_{i_{se}} = -V_i^2 \left[ \sum_{q=j,k} r_{iq} B_{se_{iq}} \cos \cos \gamma_{iq} \right] \quad (56)$$



$$P_{p,se} = r_{ip} V_i V_p B_{se_{ip}} \sin(\delta_{ip} + \gamma_{ip}); \forall p = j, k \quad (57)$$

$$Q_{p,se} = r_{ip} V_i V_p B_{se_{ip}} \cos(\delta_{ip} + \gamma_{ip}); \forall p = j, k \quad (58)$$

The equivalent series-connected voltage source model with the corresponding power injections is shown in Fig. 18.

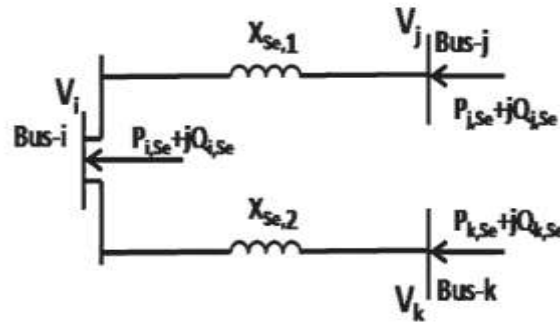


**Fig. 18** Equivalent series-connected voltage source model

The amount of apparent power supplied by the two series converters can be written as

$$\bar{S}_{se_{iq}} = \bar{V}_{se_{iq}} (\bar{I}_{iq})^* = jr_{iq} V_i B_{se_{iq}} e^{j(\delta_i + \gamma_{iq})} (\bar{V}_{iq} - \bar{V}_q)^* \quad \forall q = j, k \quad (59)$$

Substituting Equations and solving for the supplied power,

$$P_{se_{iq}} = r_{iq} V_i V_q B_{se_{ip}} \sin(\delta_{iq} + \gamma_{iq}) - r_{iq} V_i^2 B_{se_{iq}} \sin \gamma_{iq}; \forall q = j, k \quad (60)$$

$$Q_{se_{iq}} = -r_{iq} V_i V_q B_{se_{iq}} \cos(\delta_{iq} + \gamma_{iq}) - r_{iq} V_i^2 B_{se_{iq}} \cos \gamma_{iq} + r_i^2 V_i^2 B_{se_{iq}}; \forall q = j, k \quad (61)$$

$$P_{se_{iq}} = r_{iq} V_i V_q B_{se_{ip}} \sin(\delta_{iq} + \gamma_{iq}) - r_{iq} V_i^2 B_{se_{iq}} \sin \gamma_{iq}; \forall q = j, k \quad (62)$$

$$Q_{se_{iq}} = -r_{iq} V_i V_q B_{se_{iq}} \cos(\delta_{iq} + \gamma_{iq}) - r_{iq} V_i^2 B_{se_{iq}} \cos \gamma_{iq} + r_i^2 V_i^2 B_{se_{iq}}; \forall q = j, k \quad (63)$$

### B.2 SHUNT CONNECTED VOLTAGE SOURCE MODEL

The shunt-connected voltage source can be modeled as an equivalent power injection from the GUPFC shunt branch to the series branches through converters 1 and 2. This model is also used to provide the converter switching losses. The reactive power injection at the shunt converter is used to control/ maintain the voltage level at the sending end to within

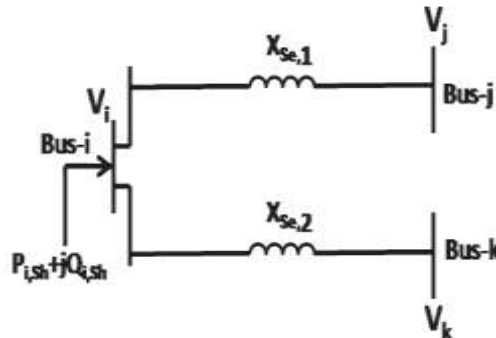


**Fig. 19** Equivalent shunt-connected voltage source model

the necessary limits. The equivalent shunt- connected voltage source model with the corresponding power injections is shown in Fig. 19. The total switching losses in one converter are about 0.8–1% [36,64] of the power transferred through the converter. If these losses are considered, then the real power injection of the shunt converter is

$$P_{sh} = -1.03 \left( \sum_{q=j,k} P_{se_{iq}} \right) \quad (64)$$

### B.3 EQUIVALENT GUPFC MODEL

The final steady-state GUPFC power injection model is obtained by combining the series-connected voltage and shunt-connected voltage source models. The equivalent GUPFC model is shown in Fig. 2. The resultant power injections are given by

$$P_{i,GUPFC} = P_{i,se} + P_{sh} \quad (65)$$

$$Q_{i,GUPFC} = Q_{i,se} + Q_{sh} \quad (66)$$

Similarly, the GUPFC power injections at the  $j$  and  $k$  buses are solely from the series voltage sources, as the shunt branch has no effect.

#### B.4 MODIFICATIONS TO THE JACOBIAN ELEMENTS

The Jacobian elements in the Newton–Raphson iterative process can be modified using the following equations

$$H^{new} = H^{old} + H' \quad (67)$$

$$H'_{ii} = \frac{\partial P_{i,GUPFC}}{\partial \delta_i} = -1.03 \times (Q_{j,gupfc} + Q_{k,gupfc}) \quad (68)$$

$$H'_{qq} = -Q_{q,GUPFC}; \forall q = j, k \quad (69)$$

$$H'_{iq} = H'_{qi} = Q_{q,GUPFC}; \forall q = j, k \quad (70)$$

Similar modifications can be applied for other Jacobian elements.

#### B.5 MODIFICATIONS TO THE POWER MISMATCH EQUATIONS

The power mismatch equations in the Newton–Raphson method can be modified using the following equations:

$$P_{i,new} = P_{i,old} + P_{i,GUPFC} \quad (58)$$

$$Q_{i,new} = Q_{i,old} + Q_{i,GUPFC} \quad (59)$$

where  $\square P_{i,old}$  and  $\square Q_i$  are the power mismatches without the GUPFC device. Similar modifications can be obtained for the remaining GUPFC buses.